

A Bevalac Calibration of a Scintillating Optical Fiber Hodoscope for Possible use on the Advanced Composition Explorer (ACE)

W.R. Binns¹, D.J. Crary¹, A.C. Cummings²,
J. Klarmann¹, D.J. Lawrence¹, and R.A. Mewaldt²
1. Washington University, St. Louis, MO, USA;
2. Caltech, Pasadena, CA, USA.

ABSTRACT

As part of instrument definition activities for the Advanced Composition Explorer (ACE) we are evaluating a hodoscope comprised of scintillating fibers for possible use in the Cosmic Ray Isotope Spectrometer (CRIS). The hodoscope would determine the trajectories of individual cosmic ray nuclei which stop in the silicon solid state telescopes in CRIS. We report a preliminary analysis of data from a Dec., 1990 Bevalac calibration of a CRIS test model which consisted of a scintillating fiber hodoscope, utilizing 200mm, square cross section scintillating fibers, and silicon detectors for $dE/dx-E_{Tot}$ measurements. The positional resolution obtained in our preliminary data analysis is $\sim 60\mu\text{m}$ for angles from $0-30^\circ$. The detection efficiency for iron and silicon nuclei was determined to be $>99\%$ for beam angles of $\geq 20^\circ$.

1. Introduction: The use of scintillating optical fibers for precise trajectory measurements of charged particles is relatively new and the technique continues to be developed. They offer the advantages of high position resolution (Davis, et al., 1989) and low mass; no pressure vessel is required, and they can be fabricated into hodoscopes which cover large areas. They are presently being used in the Scintillating Optical Fiber Isotope Experiment (SOFIE)(Connell et al., 1990; Binns, 1987) which is to be flown on a high altitude balloon in Aug, 1991, and are being planned for use in the Large Isotope Spectrometer for Astromag (LISA) (Binns et al, 1990). In this paper we report preliminary results of a Bevalac study aimed at the possible use of scintillating fibers in the CRIS experiment on ACE (Stone, et al., 1990).

2. Experiment: An instrument consisting of a fiber hodoscope and silicon $dE/dx-E$ detectors arranged as shown in Fig. 1 was exposed to charged particles at the Lawrence Berkeley Laboratory Bevalac accelerator. Four x,y planes of fibers were used; three planes were located in front of the silicon detectors and one was interleaved in the silicon detector stack. The fiber ribbons were constructed using $200\mu\text{m}$ square cross-section fibers bonded with Uralane adhesive to a kapton substrate. The three fiber planes H1, H2, and H3 were each spaced by 3 cm and had active areas of 18 cm x 10cm, 16 cm x 10 cm, and 10 cm x 10 cm respectively. The fiber output area was $250\mu\text{m} \times 92\text{ cm}$, with the extra $50\mu\text{m}$ over the fiber size being taken up by adhesive. The output was divided into "tabs" with length 1.6 cm. The tabs were then stacked to form a rectangular output with approximate area 1.6 cm x 1.5 cm which was viewed by an image intensified CCD camera (ITL MCP-225 dual MCP intensifier; Thompson TH-7866 CCD camera). Each fiber projects onto approximately 6 (horizontal.) x 3 (vertical) pixels on the CCD array, with the pixel size being $16\mu\text{m}$ wide by $27\mu\text{m}$ high. The image intensifier output is proximity focused onto the CCD array using a fiber optic reducer with a demagnification factor of 0.45 ± 0.005 . Thus one pixel width

corresponds to about $36 \mu\text{m}$ in fiber space. A particle traversing all four fiber planes should result in eight pixel "clusters" which "light up", each cluster corresponding to one x or y coordinate. The address and signal (8 bits) for each pixel above discriminator level is then read out along with the five silicon detector pulse heights. The silicon detectors had diameters of 6 cm with the front three detectors each having thickness 3 mm and the two rear detectors each having thickness 1.7 mm. The silicon detectors were offset laterally as shown in Fig. 1 so that particles with wide angle trajectories would traverse all 5 detectors.

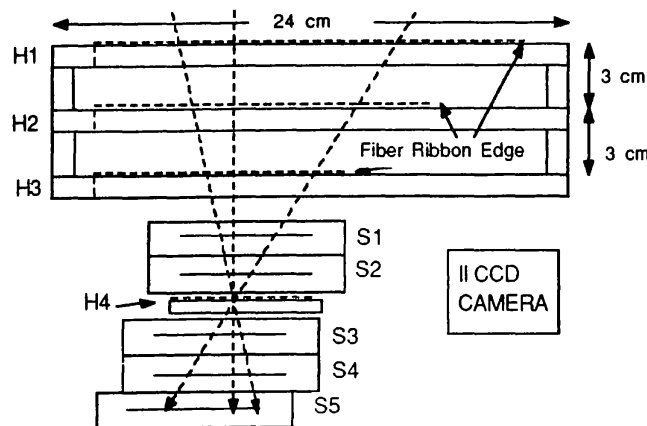


Fig. 1--Instrument cross section top view.

low energy stopping, and high energy iron and silicon nuclei for angles varying from -10° to 40° . These data have been used to study the position resolution, the angle resolution, and the detection efficiency of the fiber trajectory detector. The mass resolution obtained using the silicon detectors has not yet been determined in this preliminary analysis.

3. Data Analysis and Results--For each pixel cluster, a coordinate centroid in x and y on the CCD pixel array was calculated. Fig. 2 shows a plot of centroids as viewed by the pixel array. The locus of centroid points for a given tab is clearly separated from adjacent tabs, thus clearly identifying the tab penetrated by that particle. On the other hand, within a tab the centroids are not clearly separated. This results from the optical coupling of the fibers in the detector active area.

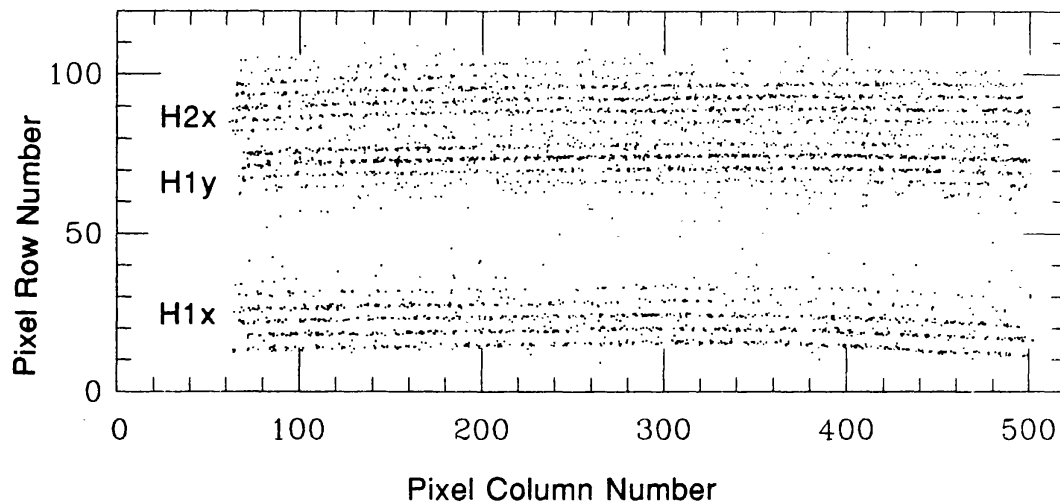


Fig. 2--Coordinate centroids in CCD-pixel space for iron events.

To study the position and angle resolution, we selected events by requiring at least one pixel cluster in each of the 6 layers of H1, H2, and H3, and employed the method of residuals (Davis, et al. 1989) to determine the positional resolution obtained in the x-coordinate of the first three hodoscope planes. In this method a straight line connects the H1 and H3 centroid positions on the pixel array for a particular event (See inset in Fig. 3). The H2 centroid position deviation from the intersection of the straight line with the H2 plane (Δx) is then calculated for each event and histogrammed. The resolution in position for a single coordinate, σ_x , can be shown to be equal to $\sigma_x = (2/3)^{1/2} \sigma_{\Delta x}$, where $\sigma_{\Delta x}$ is the rms deviation of the Δx distribution, assuming that the resolution in each of the three planes is the same (Davis et al., 1989). Fig. 3 shows Δx distributions for particles traversing H_{1x}, H_{2x}, and H_{3x} after a first order correction is applied for a variable magnification resulting from a "pincushion" image distortion in the fiber reducer. The beam was approximately circular with a beam diameter of ~5 cm and was at angles of 0° and 30° with respect to the normal to the fiber planes. The standard deviations (rms) of the distributions are $\sigma_{\Delta x} = 72$ and $68 \mu\text{m}$, giving coordinate resolutions of $\sigma_\theta = 58$ and $55 \mu\text{m}$ for 0° and 30° inclination angles respectively. It should be emphasized that this resolution was obtained using particles over the full beam diameter of 5 cm without applying any mapping corrections for fiber straightness or nonparallelism of fiber ribbons from plane to plane, and without selecting particles of a particular charge.

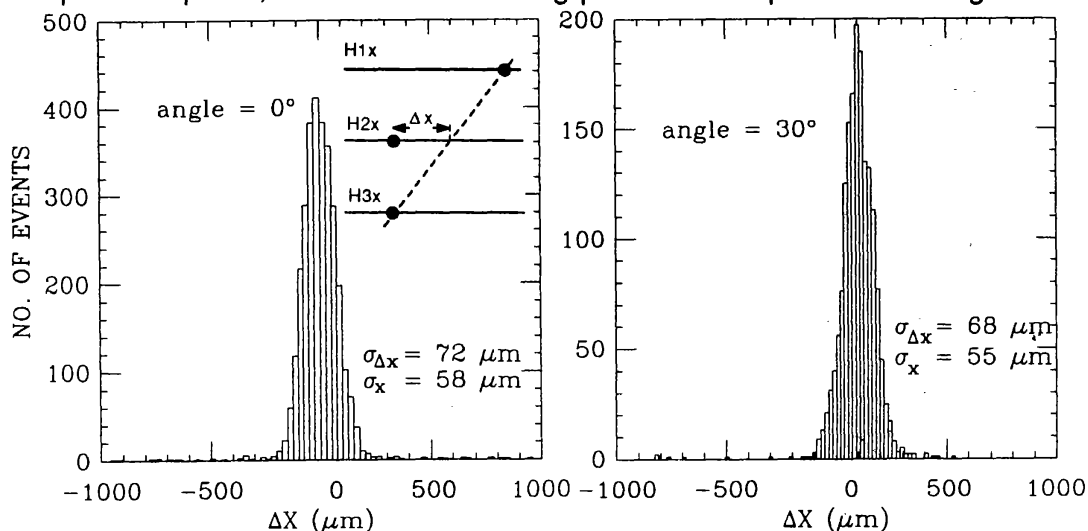


Fig.3-- Δx distributions for 0° and 30°.

Fig. 4 shows the distribution of angles obtained by doing a least squares fit to the three coordinate pairs for each particle. The resolution in angle gives $\sigma_\theta = 0.55^\circ$, considerably broader than can be accounted for by the measured position uncertainty. This resolution in angle is essentially the same for all three angles. We believe that this represents a combination of the real divergence angle of the Bevalac beam and scattering in the material in front of the detector. We can correct for this in our continuing data analysis by applying angle corrections on a particle by particle basis. This should result in improved mass resolution for wide angle particles.

We have also used our data to measure the detection efficiency of the fiber detector for both iron and silicon nuclei incident at various angles. To measure the detection efficiency we selected events with good hodoscope

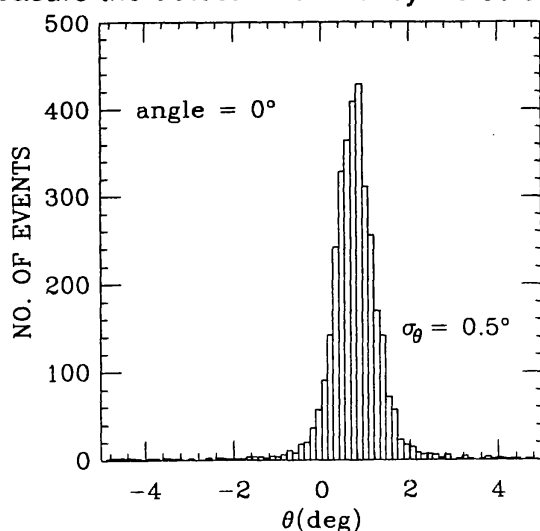


Fig.4--Angle distribution for 0° run.

signals in H_{3x} and H_{3y} . Additionally we selected noninteracted Fe or Si events using the silicon $dE/dx-E$ detector signals. For these events we then looked at planes H1 and H2 to see the fraction of selected events that gave good signals in H_{1x} , H_{1y} , H_{2x} , and H_{2y} . The following table lists the detection efficiencies obtained for fiber planes H1 and H2. We see that for iron, the efficiencies exceed 99% for all angles. For silicon, the efficiencies are $\geq 98.6\%$, with the exception of the zero

Angle	Plane no.	Fe		Si	
		x	y	x	y
30°	1	99.7%	100%	98.6%	98.6%
	2	100	100	100	100
20°	1	99.8	99.1	98.9	98.9
	2	99.8	99.8	100	98.9
0°	1	--	99.3	--	96.0
	2	99.3	99.3	96.8	99.2

degree inclination angle run. A small reduction in efficiency may be expected at very small angles since the fiber cladding thickness is 10 μm , thus separating the active core scintillator material in adjacent fibers by 20 μm .

4. **Conclusions:** We have shown that the fiber detector tested at Bevalac obtained resolution in position of $\sim 60\mu\text{m}$ over an area of ~ 5 cm diameter using 200 μm fibers. This is at least a factor of two better than is required for ACE. In addition we have demonstrated a detection efficiency of $\sim 99\%$ for iron and silicon nuclei.

5. References

- Binns, W.R., (1987) in "Genesis and Propagation of Cosmic Rays", Ed. M.M. Shapiro and J.P. Wefel, NATO ASI Series C, **220**, 391.
- Binns, W.R., et al., (1990) in AIP Conf. Proc., Ed. Jones, Kerr, and Ormes **203**, 83.
- Connell, J.J., et al. (1990) Nuc. Instr. and Meth. in Phys., **A294**, 335.
- Davis, A.J., et al. (1989) Nuc. Instr. and Meth. in Phys., **A276**, 347.
- Stone, E.C., et al. (1990) in AIP Conf. Proc., Ed. Jones, Kerr, and Ormes **203**, 48.

6. **Acknowledgements:** This experiment would not have been possible without the important contributions of P.F. Dowkontt and J.W. Epstein in the instrument development for this work. This work was supported in part by NASA grants.